

Mathematical model and numerical simulations of the migration and growth of Biscay Bay anchovy early larval stages

Ahmed BOUSSOUAR^a, Soizick LE BIHAN^{b,c*}, Ovide ARINO^c, Patrick PROUZET^d

^a UPPA, Laboratoire de mathématiques appliquées, 64000 Pau, France

^b Ensar, Laboratoire halieutique, 65, rue Saint-Brieuc, 35042 Rennes, France

^c IRD, Geodes, 32, avenue Henri-Varagnat, 93143 Bondy cedex, France

^d Ifremer, Laboratoire halieutique d'Aquitaine, Technopole Izarbel, Maison du parc, 64210 Bidart, France

Abstract – The paper presents a mathematical model of the early larval stage, from spawn to the resorption of the yolk-sac, of the anchovy, *Engraulis encrasicolus*, of the Bay of Biscay. The model describes the temperature-dependent growth and drift of passive larvae by the currents and vertical turbulence. A numerical code has been built and numerous simulations, fed by both biological (egg surveys by AZTI-San Sebastian, Spain, and IFREMER, France) and physical (circulation model by IFREMER-Brest, France) data, were undertaken. Their main features are presented and discussed here, and some conclusions on the possible utilization of the results in improving estimates of anchovy stocks by the daily egg production method are drawn. © 2001 Ifremer/CNRS/IRD/Éditions scientifiques et médicales Elsevier SAS

Résumé – Modèle mathématique et simulations numériques des processus de croissance et migration du stade passif de la larve d'anchois du golfe de Gascogne. L'article présente un modèle mathématique de la première phase du stade larvaire, de la ponte à la résorption du sac vitellin, de l'anchois, *Engraulis encrasicolus*, du golfe de Gascogne. Le modèle décrit la croissance de la larve en fonction de la température et son entraînement passif par les courants et la turbulence verticale. Un code numérique a été mis au point et de nombreuses simulations numériques ont été faites, nourries par des données biologiques (fournies par Azti-San Sebastian, Espagne, et Ifremer, France) et physiques (fournies par Ifremer-Brest). Les principaux résultats issus de ces simulations sont présentés et discutés ici, et quelques conclusions sont tirées quant à leur utilisation éventuelle pour, par exemple, améliorer les estimations sur les stocks d'anchois faites à partir des estimations sur la ponte journalière. © 2001 Ifremer/CNRS/IRD/Éditions scientifiques et médicales Elsevier SAS

anchovy / growth / migration / numerical simulation / passive stage

anchois / croissance / migration / simulation numérique / stade passif

1. INTRODUCTION

Marine fish populations, in particular pelagic ones, can be characterized by important abundance fluctuations (Lasker and MacCall, 1983; Valvidia, 1978). Conse-

quences of such fluctuations are dramatic for countries where the exploitation of these resources is crucial for the economy.

Even if clupeoid populations are affected by high fishing pressure, their abundance variability is also known to respond to climatic variability (Kawasaki, 1983; Pauly and Tsukayam, 1987; Payne et al., 1987).

It is now admitted that ocean conditions influence recruitment success and early stage survival. A number of

*Correspondence and reprints: fax: +33 2 23 48 55 35.
E-mail address: slebihan@ird.fr (S. Le Bihan).

authors elaborated around this issue, starting with the pioneering critical period hypothesis by Hjort (1914, 1926). More recently, Cushing (1975) formulated the match-mismatch theory, an extension of Hjort's view, and Lasker (1978) put forward his ocean stable hypothesis. Bakun (1985) found convincing evidence that the spawning peak of pelagic fishes in upwelling areas coincides with a seasonal minimum in offshore Ekman transport (see also a recent monograph by Bakun (1996) and other publications by this author quoted therein). Other studies can also be quoted (Blaxter and Hunter, 1982; Cushing, 1982; Lasker, 1985; Borja et al., 1996) for the Bay of Biscay area, as works relating to the recruitment of clupeoids with environmental conditions in upwelling areas. Leggett and Deblois (1994) made a thorough review of the literature with regards to the evaluation and comparison of the following two hypotheses: 1) that year-class strength be determined by mortality during the pre-juvenile stage of the life history; 2) that recruitment in marine fishes be regulated by starvation and predation in the egg and larva stages. The work of Cury and Roy (1989) has had the greatest impact in recent years; they coined the expression of environmental 'window' to mean a small interval of the wind speed range, for example, which is most favorable to the success of recruitment.

But the complexity of the relationship between environmental conditions and recruitment as well as the lack of data make this relationship far from being completely modelled (Cole and McGlade, 1998).

While discussions based on data have flourished on this subject, mathematical models which could capture a sufficient dose of biological and physical realism are very few. As far as we know, the most advanced results along this line are due to Wroblewski and coworkers (1984, 1987, 1989) who, however, dealt with very simplified models. In contrast, we aimed to describe fish dynamics by a rather detailed model. Indeed, we propose a numerical simulation model which, fed by biological and oceanographical data, gives a sort of virtual laboratory in which it would be possible to mimic the main dynamic processes governing the evolution of the Bay of Biscay anchovy, *Engraulis encrasicolus*. The model describes the early larval stage of the anchovy, the period ranging from spawn to the resorption of the yolk-sac, which is both a period of endogenous feeding and passive transportation.

The model is made up of three components: a demographic expression involving birth and mortality; a biological term which describes individual growth depicted in terms of the progression of the larvae through developmental stages; and a physical term which describes the drift of larvae by water currents. The state variable for the dynamics of the larvae is the density of larvae, $l = l(t, a, s, P)$, where, at any chronological time t , a denotes the age, s the location within the stages, and $P = (x, y, z)$ represents a generic point in the physical space.

So, the instantaneous rate of variation of the density with respect to time, $\partial l / \partial t$, is balanced by the sum of three algebraic quantities:

– the demographic flux rate

$$- \mu(a, s, t, P)l - \frac{\partial l}{\partial a}$$

– the biological flux rate

$$- \frac{\partial(fl)}{\partial s}$$

where the variable s may take any value from $s = 1$, which corresponds to the date of spawning, to $s = 12$, which corresponds to the end of the yolk-sac stage, and the function $f = f(T, s)$ gives the instantaneous growth rate of progression within the stages, dependent upon the temperature T . We will come back to this in section 2.2.

The physical flux rate determined in terms of the 3-D current velocity $\vec{V}(t, P)$ and the mixing coefficient $h = h(t, P)$ gives

$$- \text{div}(Vl) + \frac{\partial}{\partial z} \left(h \frac{\partial l}{\partial z} \right)$$

With the above parameters, the equation for the variation of l reads

$$\frac{\partial l}{\partial t} = - \frac{\partial l}{\partial a} - \mu(t, a, s, P)l - \frac{\partial(fl)}{\partial s} - \nabla \cdot (l\vec{V}) + \frac{\partial}{\partial z} \left(h \frac{\partial l}{\partial z} \right)$$

2. MATERIALS AND METHODS

2.1. Precisions

2.1.1. Initial conditions

Initial conditions are given at $t = 0$ (beginning of the year). In the Bay of Biscay, anchovy reproduction takes

place from April to roughly the end of July (Motos, 1996). For anchovies, the larval stage lasts for at most 2 months (Mullin, 1993). Therefore, we are justified in assuming that no reproduction takes place at the beginning of the year and no larva survives until the end of the year, so that there is no larva alive at the beginning of the year,

$$l(0, a, s, x, y, z) = 0$$

2.1.2. Vertical boundary

Vertical boundary conditions are imposed at the surface and at the seabed. With the rigid lid assumption, the vertical component of the velocity is zero at the sea surface. This condition reads

$$h \frac{\partial l}{\partial z} = 0 \text{ at } z = 0,$$

The condition at the seabed reads

$$h \frac{\partial l}{\partial z} = 0 \text{ at } z = -\Psi(x, y) \text{ with } \Psi \text{ as the depth.}$$

2.1.3. Lateral boundary conditions

The lateral boundary is the part of the physical boundary apart from the sea surface and the seabed. Since the equation is a first-order transport in the horizontal variables, if we assume that reproduction takes place in the interior of the domain, there will be a positive lower limit to the time needed for any larva to reach the lateral boundary. Part of the lateral boundary, for example the offshore limit, will not be reached by the time the larva ends its cycle. On the other hand, the coastal boundary is likely to be within reach of some of the larvae. A possible way of accounting for the exchanges at this boundary could be imagining a virtual 'exit' compartment, to assume that the larvae leaving the domain by those coastal boundaries, where and as long as the component of the current normal to those boundaries is directed outward, go to this 'exit' compartment. They return from it to the domain through the same boundaries when the direction of the current changes to inward. This, however, would require a careful inspection of the coastal currents. Leaving this for further studies, we simply assumed here that no material goes through the lateral boundaries.

2.2. Data setting

2.2.1. Biological data setting

2.2.1.1. Eggs

Biological data were extracted from egg surveys performed by the AZTI and IFREMER (Motos et al., 1998). Each annual survey consists of sampling made from a boat which, once a year, during 10 to 15 d, during the spawning season period in May or June, goes over the whole Bay of Biscay to look for anchovy eggs. Transects of the egg survey are on latitudinal lines, when starting from the French coast, and on longitudinal lines when starting from the Spanish coast. The distance between two contiguous transects may vary, depending on the found densities.

Thus, the grid for biological survey ranges from 43.2 to 46.1 latitude and from 1.2 westward to 4.4 longitude and is split into cells of 3×15 squared nautical miles (in some case, the cell side is cut in half: 3×7.5 squared nautical miles).

The data involved here are for the year 1994 with 431 stations, and for the year 1996 with 320 stations. The survey stops when no eggs are found on two consecutive transects.

For the simulations, it was arbitrarily assumed that the initial egg distribution inside the water column was: 25 % of the eggs are uniformly distributed in the interval ranging from 6.5 to 7.5 m deep; 50 % are uniformly distributed between 7.5 and 8.5 m deep; and 25 % are uniformly distributed within 1 m below 8.5 m (Garcia and Palomera, 1996).

It remains to be seen how the data on eggs are converted into inputs for the model. The strategy employed here is to group together the eggs of three ages, multiplying the total number of eggs by a correction coefficient accounting for the possible mortality over the 3 d of an egg's life. The correction formula reads as follows:

$$\frac{\text{egg}_0 + \text{egg}_1 + \text{egg}_2}{1 + \exp(-\mu t_1) + \exp(-\mu t_2)}$$

where the notation egg_i represents the number of eggs aged i days present in the cell, and t_j , $j = 1$, or 2 , the duration in days, elapsed from the time of spawning. For eggs aged 1 d, it is $t_1 = 1$, and $t_2 = 2$ for eggs aged 2 d.

More generally, t_j is to be expressed in terms of the time unit used for the mortality rate μ , which here is the day.

The above formula is quite rough. It does not account for any spatial dispersion of eggs. It would be interesting to compare the results obtained using this combined method egg number with those that could be obtained by taking the eggs aged 0 d only.

Data are expressed in terms of a number of eggs per square meter, in accordance with the sampling method that counts together the eggs which belong to the same right cylinder of the water column.

A crucial assumption is that the daily distribution is the same throughout the scientific season. Of course, this assumption is certainly wrong and is just the consequence of the egg sampling procedure. Only one egg sampling survey has been performed each year, and it is roughly assumed that the distribution found during this survey is a faithful image of what is going on every day during the time of the survey. From a methodological point of view, this is not a big problem and can be overcome as soon as additional data will become available. Combined with the assumed constant mortality rate, also incorrect, and the fact that no escape of larvae at the lateral boundaries is allowed, it gives at least and at most a rare opportunity to compare the sole effect of temperature and oceanic currents and turbulence on growth and distribution of larvae, independently of all other demographic or whatever factors.

2.2.1.2. Larval growth

As already mentioned, larval growth is determined as a function of the temperature. The growth model is made up of two sub-models: the first one encompasses the period going from fertilization to hatching. Such a model was first proposed in the study of California anchovy, *Engraulis mordax* (Lo, 1985). The period of egg development is divided into eleven stages established by Moser and Ahlstrom (1985), and the model provides the age of the egg at each of those eleven stages as a function of the temperature. It is a parametric model with three parameters. For the Bay of Biscay anchovy, *Engraulis encrasicolus*, Motos (1994) determined the parameters in laboratory experiments.

$$y_{i,T} = 15.45 \exp(-0.1145T + 0.0098i) i^{1.74}$$

Hatching occurs at the end of the eleventh stage, which, depending on the temperatures crossed by the egg throughout its development, will occur more or less rapidly.

The second sub-model deals with the period going from hatching to the end of the yolk-sac, that is to say, still a period, counted as a twelfth stage, when the larva does not depend on the environment for its living. The duration of this stage is given by a function of the type:

$$D_v = ET^{-F}$$

where, as for the previous stages, the parameters E , F and D_v are determined in laboratory, at constant temperatures. This information is to be converted into instantaneous variation of stage.

We obtain the expression of maturity in stage i at time t

$$m_i(t) = \int_{t_i}^t \frac{1}{D_i(T(s))} ds$$

the completion of the stage corresponding to the time t for which $m_i(t) = 1$ and i is the stage and T the temperature.

It is this formula that is used to describe the progression in the yolk-sac stage, with the function D_v taken from Motos (1994). The formula obtained by Motos however is not specific of the yolk-sac stage: it covers the whole passive stage, from egg fertilization to the end of the yolk-sac stage, or, in other words, the endogenous feeding period. In the absence of a specific model for the yolk-sac stage, this was considered a possible choice. This choice is of course disputable: the parameters computed in this manner account for the whole growth process from fertilization to the end of the yolk-sac stage, wherein the specificity of the yolk-sac stage is likely to be dampened. The values of the parameters determined by Motos (1994) are $E = \exp(10.376)$ and $F = 2.1749$ (figure 1).

The two models were combined together to yield a single continuous model which gives the stage (supposed to vary continuously from the value 1 to 12 with all non-integer values viewed as fractions of stages) as a function of age, at a given temperature.

It is convenient to extend the notion of stage so as to make the stage a continuous variable that was denoted s . The above formulae give the age at stage: one can invert

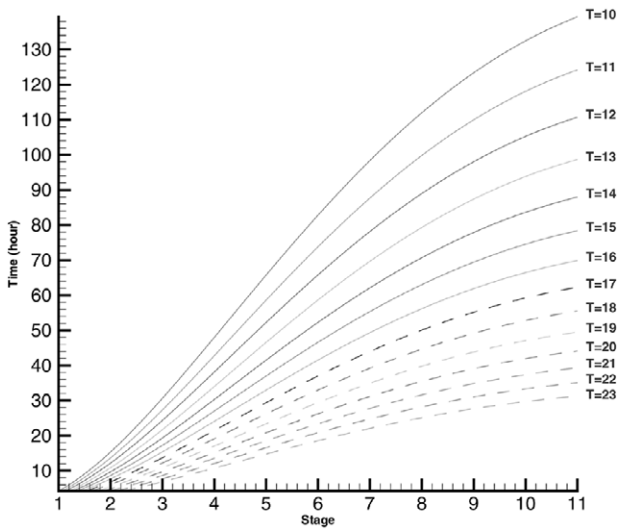


Figure 1. Exponential function relationship of stage, age based upon time and at a given temperature denoted T ($^{\circ}\text{C}$).

these formulae to determine the stage at age. Since this information has to be incorporated in a continuous time and space equation, it will be convenient to express it in terms of the instantaneous variation of the stage as a function of age and temperature.

$$\frac{ds}{dy} = \frac{\exp(-bT)}{a \exp(cs)(cs^{\alpha} + \alpha s^{\alpha-1})}$$

where $T = T(y)$ is allowed.

2.2.1.3. Demographic boundary conditions

Demographic boundary conditions are given at $s = 1$, at any time during the spawning period:

$$l(l,t,P) = B(t,P)$$

The function $B(t,P)$, equal to 0 for $t < t_0$, where t_0 is day 1 of spawning, is positive during the spawning period and periodic in t with a period equal to 1 d, that is to say, it is assumed that the production of eggs at any given point in the sea is the same all over the spawning period and is indeed the value extrapolated from the samples taken all over the continental shelf within a few days, treated as simultaneously gathered data. This assumption is obviously outrageously strong: the situation varies both in time and space. Although we have used a single set of data for each year, the program is organized in such a way that one could just as well feed it with several sets, corresponding to as many egg surveys.

2.2.2. Physical data setting

The physical data used in these simulations have been elaborated from the model circulation by Lazure and Jégou (1998). It is a 3-D model, which solves the Navier-Stocke's equations under hydrostatic hypothesis, and equations for the transport of heat and salt. The vertical coordinate is normalized, using sigma coordinate. The equations are solved using finite differences and a semi-implicit method. Open boundary conditions are obtained from a model on a larger domain and described variations of the sea level as a joint result of the actions tide and winds. Daily flows of the Loire and the Gironde rivers are prescribed in their respective estuary. Wind measured on the isle of Oléron is prescribed on the sea surface.

Since the main emphasis of the physical grid built up by P. Lazure and A.M. Jégou was the study of the effect of the Loire and Gironde plumes, the grid does not cover all of the Bay of Biscay. It is roughly enclosed in a pentagon spreading from 43.8 to 47.8 latitude. It follows the coastline. It ranges from 0.9 westward to 3.9 longitude and is limited offshore by the continental shelf and the 3.9 W longitude line. Along the vertical, the sigma coordinates divide the water column into ten unequal slices according to the following proportions, from the surface downwards: 0.03, 0.05, 0.1, 0.15, 0.25, 0.35, 0.5, 0.65, 0.80, 0.95. The physical cells are squares of 3×3 miles. Simulations of currents, temperature and salinity are typical for the year's range. Field data measurements are averaged over week periods, consequently, the same is true for the data computed by the circulation model.

2.3. Numerical treatment of the model

In the approximation procedure of the main equation, a finite volume scheme is utilized. The principle of such schemes is as follows: a family of meshes is selected (these are the control volumes). To each mesh, one associates an unknown number or a finite family of unknowns, inter-related by as many equations, obtained by integrating the equation on each control volume. For more details on the method, we refer to Eymard et al. (2000), Kröner (1997), Godunov (1976), Mortan (1996) and Vignal (1996). Finite volume schemes are often assimilated to finite difference schemes. However, it is not difficult to build a finite volume scheme on a triangular mesh, for example, while finite difference

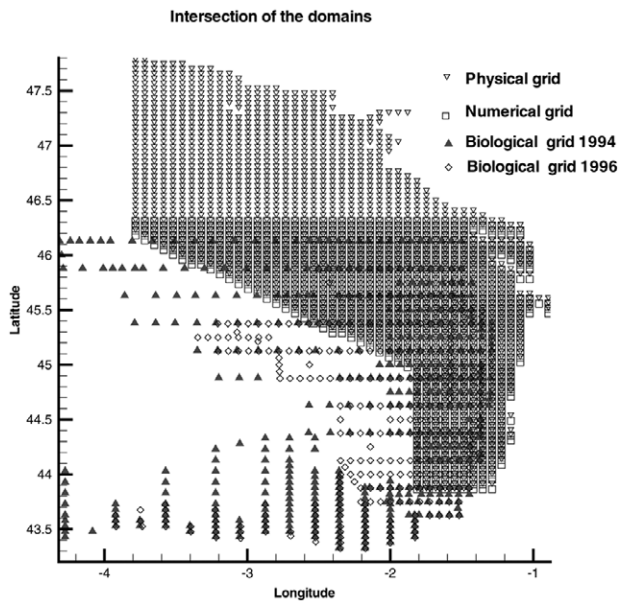


Figure 2. The physical grid and the two biological grids (1994 and 1996) are superimposed. The numerical grid is the intersection of the region delineated by physical data and biological data.

schemes are more unlikely to be extended to such meshes. In our work, we consider a mesh satisfying several hypotheses; we determine a time-step such that the Courant-Friedrichs-Levy condition (the so-called CFL condition) holds. One uses a one-sided finite difference volume scheme.

2.3.1. The domain of resolution

The domain of resolution is the intersection of two grids, the physical grid and the stations of the egg survey. The intersection of the two grids delineates a sort of polygonal region (figure 2). An important difference between the two grids is that, due to the way biological samples are taken, the grid for biological surveys is two-dimensional. Vertical diffusion as well as both vertical and horizontal transport are taken care of here. So, we used a grid of the whole volume. The mathematical representation of the volume is

$$\Omega = \bigcup_{(x,y) \in D} \{(x,y)\} \times]-\psi(x,y), 0[$$

where D is a piece of the water surface, the polygonal region determined as the intersection of the biological and the physical grids, and the function $\psi \geq 0$ is the depth of the seabed at each point (x,y) of the surface.

It is convenient in the problem under consideration to have a finer subdivision of the water column. We chose 1 m as the vertical mesh-size: completion of the vertical database was done by linear interpolation. Finally, a cell of the decomposition consists in a slab with a trapezoidal horizontal base, two vertical sides parallel to the x -axis, while the other two vertical sides are shaped by the coastline and the offshore boundary. Altogether, there are 1 140 horizontal cells; each of them is the base of a right cylinder which extends vertically from the surface down to the seabed. Each cylinder is divided along the vertical into as many slabs as the length in meters of the axis, which gives 91 532 as the total number of elementary cells.

2.3.2. Discretization procedure

The main equation has been solved numerically. The numerical scheme chosen is implicit with respect to the vertical migration (diffusion + transport), and explicit with respect to the horizontal transport and the mortality. This choice is a trade-off between time consumption and numerical accuracy (Dautray and Lions, 1988). We select a volume, and we integrate the equation on this volume over the time interval $[t_n, t_{n+1}]$. For the integration procedure, the equation is roughly divided into four groups, roughly following the subdivision into demographic, biological and physical processes:

- (I) The variation is due to growth only $\frac{\partial l}{\partial t} + \frac{\partial(fl)}{\partial s}$
- (II) The variation is due to transport only $\text{div}(Vl)$
- (III) The variation is due to vertical mixing only $-\frac{\partial}{\partial z} \left(h \frac{\partial}{\partial z} l \right)$
- (IV) The variation is due to mortality only μl

Each of these quantities is integrated over the product

$$V_{i,j,k}^{n,m} = [t_n, t_{n+1}] \times [s_{m-\frac{1}{2}}, s_{m+\frac{1}{2}}] \times C_{i,j,k}$$

We may note that the age variable does not show up: this is due to the fact that the program integrates daily cohorts. As mentioned in the discussion of data setting, the data coming from egg samples have been transformed into eggs of the day, that is, we consider that the egg sampling is providing us with the daily distribution of spawn. So, for each simulation run starting a given day with the spawn of the day as an initial value, only one time variable is needed: the variable t can be viewed indifferently as the chronological or the physiological

time. We may also observe that we do not assume any relationship between the larvae, so that in fact the whole simulation gives a collection of independent cohorts, some of them coexisting for some time. The way the data have been employed here is not the only one possible way, and several other ways could be explored with only a mild modification of the program. This will be discussed in more details in the last section of the paper.

3. RESULTS

At each time step, the program gives the density, with respect to the volume unit, of individuals of a given stage or age throughout the region covered by the simulation. As a rule, we are always looking at 1-m thick horizontal layers piled together: the water column is obtained by piling up all the layers from the surface to the bottom. A horizontal cross-section is just one such layer. A vertical cross-section piles up, from the surface to the bottom, the 1-m high bands cut along the vertical in each of the layers. Each simulation run starts from the same 0 d aged class, made up of a weighed average of the sampled eggs. Differences in the simulations are those implied by differences in the environmental conditions: current velocities, mixing coefficient, or temperature. Simulations are started on the supposedly day 1 of the spawning and are run for the next 60 d. Each daily output is saved.

During the period from spawn to the resorption of the yolk-sac, the larva is not dependent upon the environment for its feeding. It has been pointed out by several authors (for example, Hunter and Thomas, 1973) that, despite the fact that they do not need it, larvae start to look for food, essentially phytoplankton, even before yolk-sac resorption. However, one can reasonably assume that their locomotive abilities until the resorption of the yolk-sac are very low, due both to their small size, which makes the role of viscosity bigger than inertia (low Reynolds number) and also the presence of the yolk-sac which handicaps their movement. So, we assume that the larvae are essentially passive and do not feed, during the whole period covered by the simulation (see Mullin, 1993). We could in fact explore further the larval development and reach the next critical period when the larva starts to use its swim-bladder. This would not involve any change in the model, especially if we assume that the larva is still passive during the transition to the stage when the swim-bladder is fully functional.

3.1. Dispersion of the eggs within the water column – Impact of vertical diffusion

Simulations have been undertaken to determine the role of vertical diffusion. *Table I* shows the values obtained from

Table I. Simulations with/without diffusion for the same initial egg distribution.

Total depth (133 m)	Initial condition ($t = 0$) (larva·m ⁻³)	No mixing ($t = 1 \text{ h } 7 \text{ min}$) (larva·m ⁻³)	Mixing ($t = 1 \text{ h } 7 \text{ min}$) (larva·m ⁻³)
-1	0	0	47.57
-2	0	0	47.58
-3	0	0	47.52
-4	0	0	47.39
-5	0	0	47.17
-6	0	0	46.88
-7	179.30	145.80	46.50
-8	358.61	319.50	46.00
-9	179.30	205.85	45.32
-10	0	35.66	44.37
-11	0	3.80	43.05
-12	0	0.31	41.10
-13	0	0.02	37.86
-14	0	< 0.01	32.51
-15	0	<< 0.01	26.26
-16	0	<< 0.01	20.32
-17	0	<< 0.01	15.05
-18	0	<< 0.01	10.63
-19	0	0	7.16
-20	0	0	4.58
-21	0	0	2.78
-22	0	0	1.61
-23	0	0	0.88
-24	0	0	0.45
-25	0	0	0.22
-26	0	0	0.10
-27	0	0	0.04
-28	0	0	0.02
-29	0	0	0.01
-30	0	0	<< 0.01
-31	0	0	<< 0.01
-32	0	0	<< 0.01
-33	0	0	<< 0.01
-34	0	0	<< 0.01
-35	0	0	<< 0.01
-36	0	0	<< 0.01
-37	0	0	0
-38	0	0	0
-39	0	0	0
-40	0	0	0

the same initial egg distribution, after 3 h, without (column 3) and with (column 4) diffusion. Note that no egg has been found below 40 m depth and no egg is dispersed below this depth, so this part of the water column is not represented in the table. Several remarks can be made: there is a sharp difference between the no mixing and the mixing cases. Looking at the mixing case, the material disperses rather quickly and tends to become uniformly distributed within the first third of the mixed layer (above 12 m depth). There is a rather pronounced drop in density between 12 and 16 m deep, and virtually nothing below 25 m. So, the standard affirmation that the anchovies spawn near the surface makes sense. Finally, the effect of low mixing near the bottom of the mixed layer in slowing down the dispersion is clearly visible. It also shows up in the vertical cross-sections exhibited in *figure 3*.

3.2. Thermocline simulation

Whereas no boundary condition has been imposed at the top of the thermocline, only low density is found below the thermocline (*figure 3*). Thus the thermocline acts as a barrier preventing the larvae from falling down to the seabed. From the numerical computation viewpoint, it may be interesting to note that this effect has been obtained as a result of having a very low diffusion coefficient at the level of the thermocline and starting from an initial egg distribution whose support lies well inside the mixed layer. We are not assuming any type of boundary condition at the top of thermocline, and indeed we are working in the whole water column. This, in a way, can be considered a consistency test for the numerical code. There are regions where the larvae density tends to be of the same order of magnitude below the thermocline as it is above: higher concentrations of larval spread below the thermocline in the form of thin vertical digitations. A quick inspection shows that these digitations co-occur generally with the thermocline thickness becoming very small, going probably below the order of accuracy of the computations.

3.3. Distribution of larvae at the end of the yolk-sac period

3.3.1. Fraction of a 1-d cohort at a given stage, per half-day, at two different months, May and July 1996

In the two sets of graphs shown in *figure 4*, the stage distributions of an initial cohort at a succession of

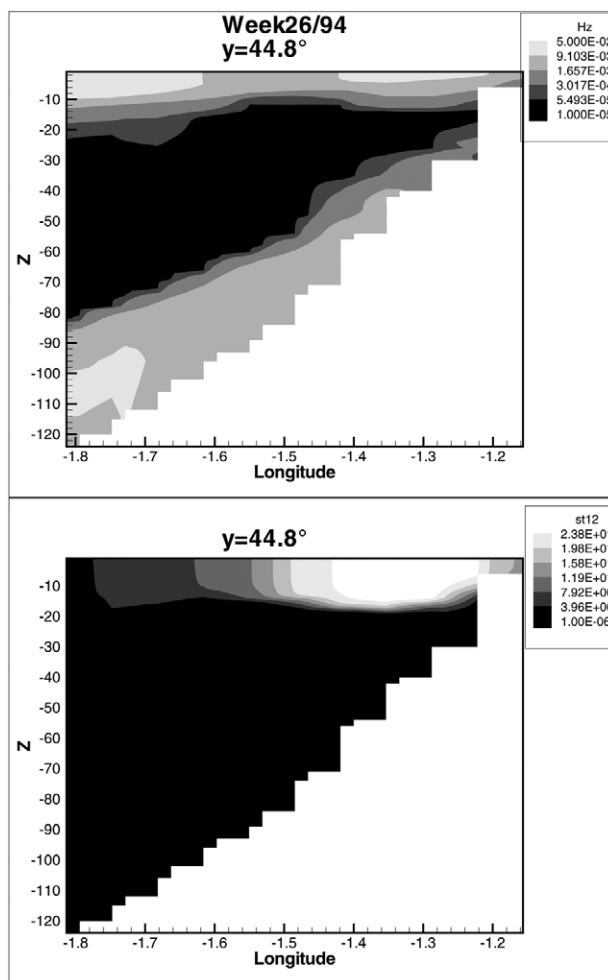


Figure 3. Thermocline effect. At the top, the mixing coefficient for week 26 of the year 1994 at the latitude $y = 44.8$. Below: cross-section of stage 12 larvae, at different depth and the longitude at given latitude $y = 45.2$. The lightest grey represents the maximum larvae density and the darker grey represents the minimum larval density.

moments of time are represented. The time step is half a day. Two curves are determined for each of the figures, one in May and one in July. A rapid inspection of the graphs shows the following: within a given month (a single cohort), there is a shift to the right, as the chronological time progresses. During the first two and a half days, the curves have a nice Gaussian shape with a single maximum, a property that does not survive beyond this time duration. After that, the curves take on several local maxima. *Figure 4* (top) shows that

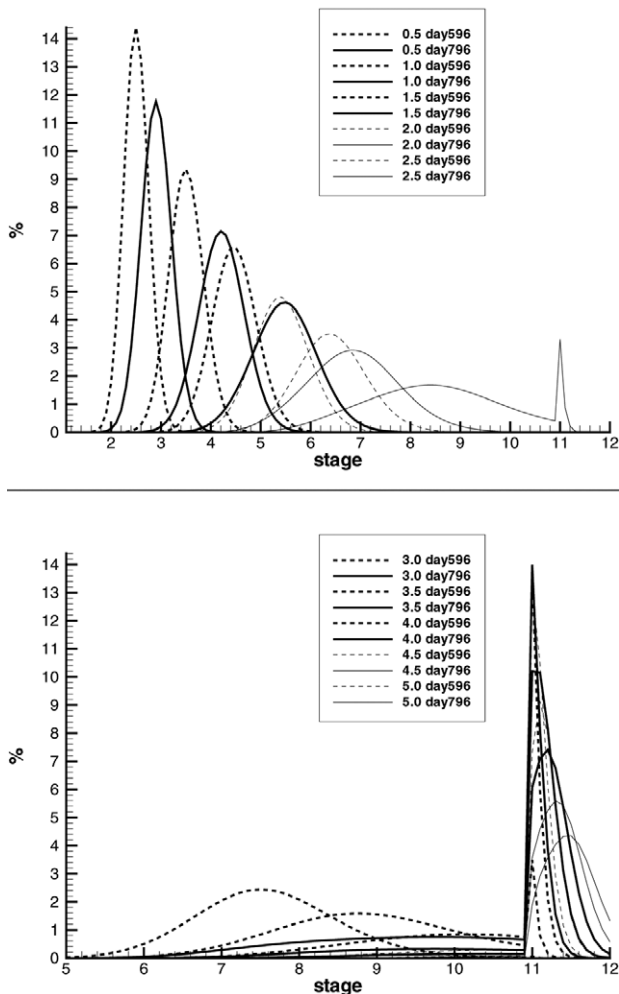


Figure 4. Fraction of the 1-d cohort at a given stage, per half-day, at two different months, May (dashed line) and July (continuous line), of year 1996.

in all cases, the larvae born in May progress slower than those born in July. Going as far as day 3.0, one can see that no larva goes beyond stage 10 through the period May-June 1996. The graph for the period July 1996 is markedly different from the one of the earlier period: larvae aged 3 d reach stage 11. Moreover, it shows that most of the larvae which survive up to this point have passed stage 11, which is in accordance with a remark often made in the literature that those larvae who survive are the stronger ones, that is, those who grow faster (Anderson, 1998; Leggett and Deblois, 1994).

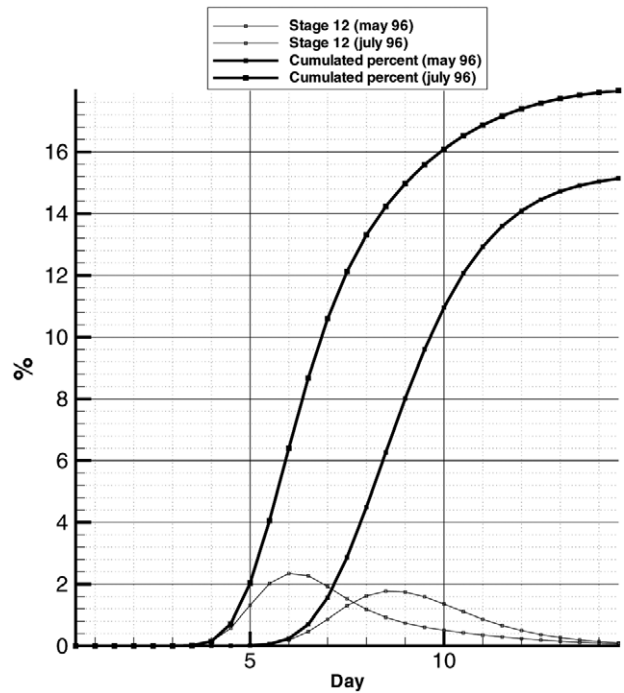


Figure 5. Fraction of larvae arriving at stage 12: per day and fraction cumulated in two different periods (May and July 1996).

3.3.2. Fraction of a 1-d cohort at the end of stage 12, per half-day, at two different months, May and July, 1996, and cumulated fraction

Figure 5 represents the fraction of an initial daily cohort arriving at the end of stage 12 on a given day, respectively in May and July 1996. While the peak in July is at day 6 and is estimated at about 2.2 %, the peak in May is at day 8.5 and is a little more than 1.8 %. Moreover, the graph for the May cohort is markedly flatter, on the left side of the peak, than the one for the July cohort which is well reflected by the graphs of cumulated percents: the first 6 % of the July cohort reach the end of stage 12 between days 4 and 6, while this happened between days 5.5 and 8.5 for the May cohort.

Survival increases with the speed at which the larvae reach the end of the yolk-sac.

As far as interpreting the curves shown in both figures 4 and 5, it may be worth pointing out that each of them has been made up of a finite number of pairs, that is to say, a number representing a stage interval (the middle of the interval) and a number giving the fraction of larvae whose actual stage lies within this interval. The gluing of

the respective points in continuous lines was just made for the sake of legibility.

3.4. Daily evolution of an age cohort

A comparison of two cohorts within a same year/within two different years (*figures 6, 7*) is realized.

Starting from the eggs spawned during a single day, throughout the whole domain covered by the simulation, the figures show the daily concentration of larvae of the same age. Two cohorts are simulated each year: one in May, the other in July, years 1994 and 1996. On each page of the layout, the four simulations are run day by day, starting from the initial egg concentrations. The first day, the fifth day and the ninth are represented in *figures 6 and 7*. As already mentioned, the daily egg production is supposed to be the same all over a same spawning season, which explains that, for day 1, we only have one picture for 1994 and one for 1996. One should also point out that the mortality rate has been assumed constant and the same all over the simulations. Consequently, differences within a year can only be explained by physical differences; moreover, comparing two simulations starting from a daily cohort of a same year, the difference in numbers between the two cohorts after a same number of days is equal to the difference between the numbers of larvae of both cohorts which have reached the end of the yolk-sac stage after these days. Recall that the physical parameters are evaluated weekly. Physical parameters of week 20/94 and week 20/96 correspond to the first week of the simulation 18/05–27/05 of years 1994 and 1996, and week 27/94 and week 27/96, corresponding to the first week of the second set of simulations. When looking at the pictures of the larvae, one should keep in mind that only larvae until the end of stage 12 are shown. More mature ones are simply not taken into account. Totalling all the stages as it is done in these simulations, the only remains of the maturation process are the overall effect of temperature on growth rate. This effect is visible on the pictures, when comparing within years: the cohort starting in July is dissipated much faster than the one starting in May (compare the pictures for 26/05/94 and 09/07/94, on the one hand, and 27/05/96 and 09/07/96, on the other hand). The temperatures at any depth or cross-section show a significant increase between May and July.

3.4.1. Cohort starting on 18/05/1994; physical data of week 20/94

We first summarize the physical data of week 20/94. An interesting feature is reflected by the picture of salinity (*figure 8*). At 5 m depth, low salinity indicates the arrival of fresh water coming from the Gironde estuary into the ocean. The water is going southward at the mouth of the river until it meets a southeast-northwest current which changes its trajectory. It then turns in the clockwise direction and starts to move in the southeast-northwest direction. The movement is even more pronounced at 10 m depth. The same movement survives at 20 m depth, although the salinity at this level is much more similar to the ocean's. Looking at the pictures of the larvae, a patch of high concentration appears near that turning point. It is distinctly visible in the last picture (ninth day).

3.4.2. Cohort starting on 01/07/1994; physical data of week 27/94

The distribution of salinity is different from what it was during week 20. While the area of very low salinity is concentrated at the mouth of the river, low salinity is clearly more extended than in May. There seems to be a trend towards less fresh water flowing from the river, while the area of low salinity spreads around and drifts southward. This might be due to the currents which are also quite different from what they were on week 20. One distinctly sees an eddy centred near the point (45.8 N, 1.8 W), turning in the clockwise direction. The temperature is very high in most of the region, and it also the highest of the four simulations. This might be the driving factor, explaining the rapid disappearance of larval concentration, the most rapid amongst the four simulations. By the ninth day of the simulation, the picture does not contain any density above 46 larvae·m⁻², while this occurs only on the last day of the simulation in May 1994 and May 1996. The comparison with the simulation of July 1996 on the eight day shows distinctly that, from an initially lower egg abundance in 1996, more larvae remain on the 9 July 96 than on the 9 July 94.

3.4.3. Cohort starting on 19/05/1996; physical data of week 20/96

The area of extension of the fresh water is significantly smaller than what it was in 1994. The current is stronger, oriented northeast-southwest along the coast and bends towards the direction southeast-northwest to the west.

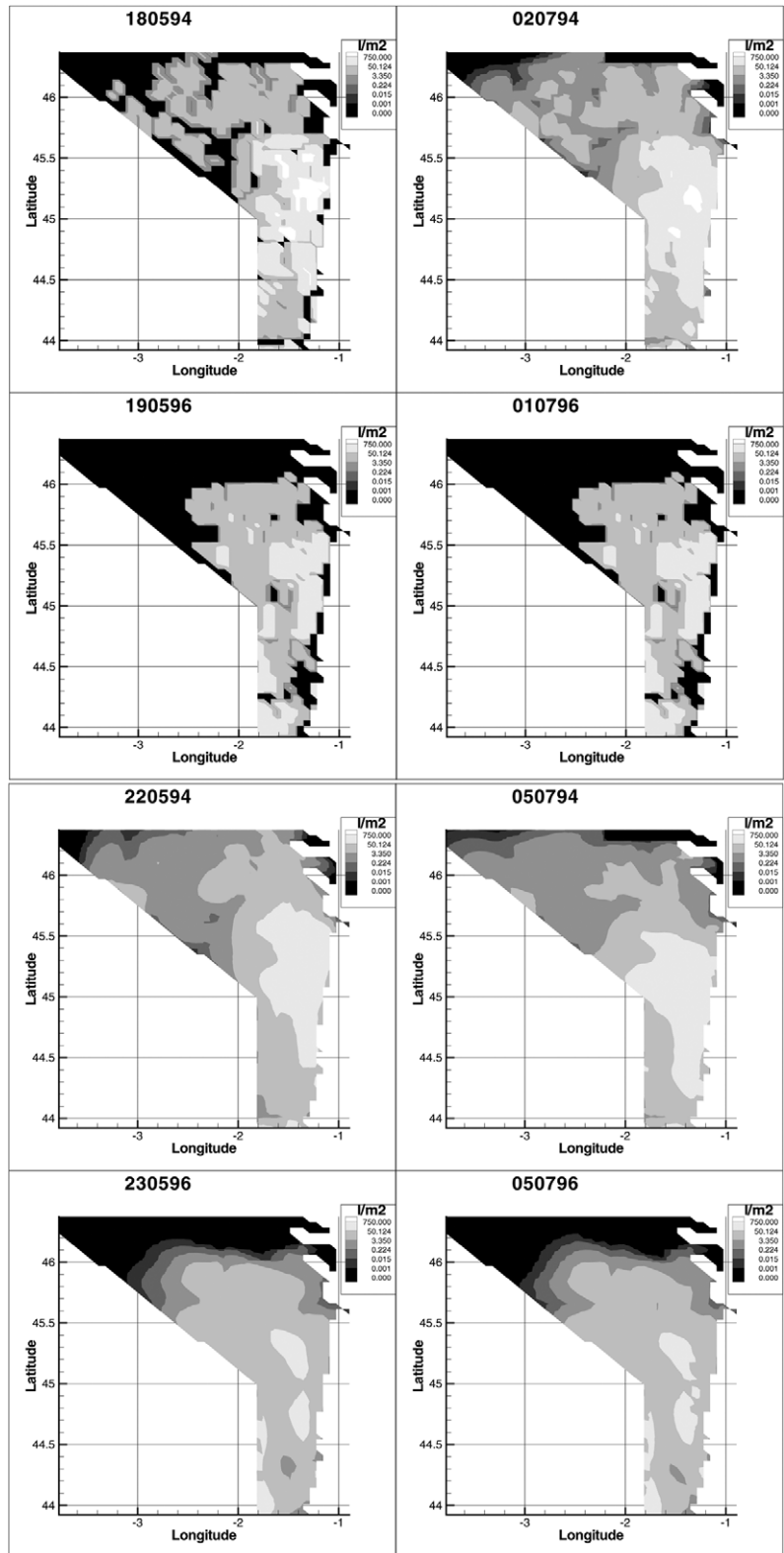


Figure 6. Daily evolution of an age cohort: comparison of two cohorts within two different years (1994 and 1996). The first and fifth day are represented. Initial egg concentrations are the one of 18 May and 1 July. For each year, initial egg distributions are identical for the starting of both months simulated.

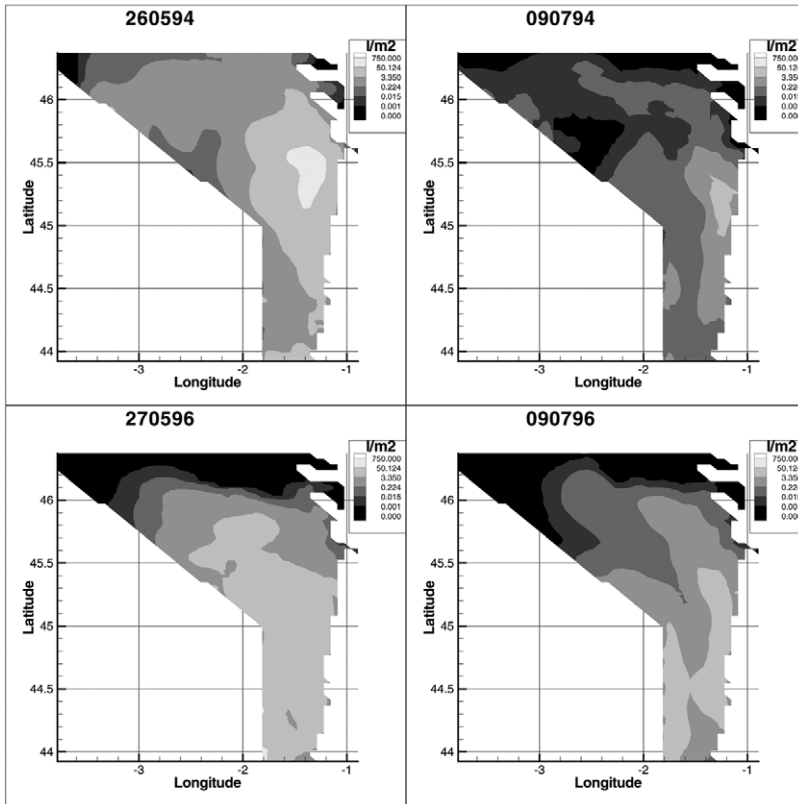


Figure 7. Daily evolution of cohort: ninth day.

There is a sharp difference in the egg abundance, which is much lower in 1996 than in 1994, and also seems to dissipate faster. The contiguous patch of eggs which spans from 44.8 up to 45.5 N latitude splits into patches of highest density, one above 45.2 N, the other below 45.1 N. The southern patch reaches the end of stage 12 faster than the other. The relative stability of the patch can be explained by the shape of the current which altogether seems to retain the material from going too southward.

Possible artefacts created by the model and its database must be underlined. One of the problems of the biological data is that they have been collected over a week and then used as if there were representative of the spawning taking place each day for the whole spawning season. One of the problems with the physical data is that the model covers only part of the Bay of Biscay. This introduces artificial boundaries for which it is just impossible to model what is going on. The choice was made to assume that there is no crossing in any direction, at the lateral boundaries. This choice does not introduce any miscount in the evaluation of the cohorts initiated in the

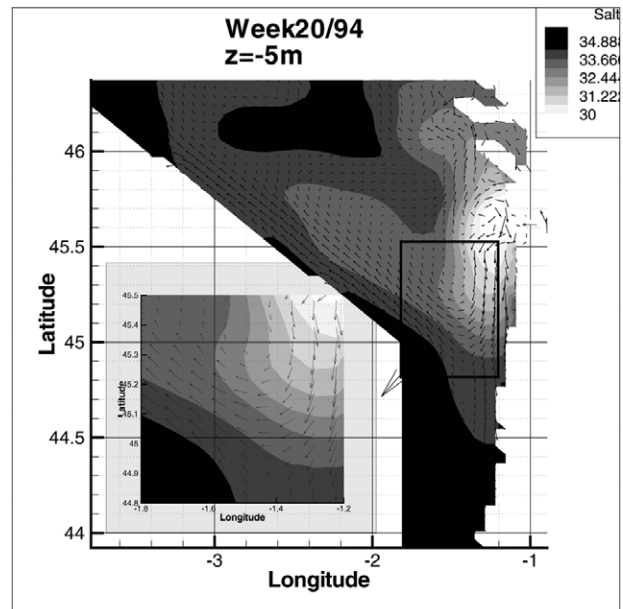


Figure 8. Physical data 1994: salinity ($\text{g}\cdot\text{L}^{-1}$) and currents for depth $z = 5$ m.

interior of the domain enclosed by these boundaries, since no density-dependence effect is accounted for until the end of the yolk-sac stage. The inconvenience of such a choice can be seen on the pictures of the larval densities in 1996. During this year, the streamlines below 45 N latitudes are directed westward and seem to hit the 1.8 W longitude line which is the limit, at these latitudes, for physical data. Egg data show high concentrations along this part of the physical contour. Since there is no possible escape for the larvae through this part of the boundary, they must stay 'stuck' there.

3.4.4. Cohort starting on 01/07/1996; physical data of week 27/96

Of the two simulations in 1996, this one shows the most rapid larval growth. One also observes that in the range 44.5–45.5 N latitude, there seems to be a persistent division into two patches, one on the western part and one on the eastern part of the map. This division even extends further to the north, as the 09/07/96 picture shows (*figure 7*). Comparing the pictures of temperature, salinity and the mixing coefficient, the only noticeable difference between the data of week 27/96 and the previous ones is in the horizontal cross-section of temperatures at 30 m depth. There is a distinctive horizontal gradient of temperature at this depth, oriented from east to west. The fact that the larvae seem to grow faster on the west side than on the east side, with a marked difference of the growth velocity in the middle tends to indicate that a significant proportion of the larvae can be found in the 30–40 m depth. Again, the currents going southward along the coast, then turning westward to go northward along the western boundary may also be responsible for part of the dispersion of the larvae located initially near the coast. We also note that the concentration of larvae drops significantly between the seventh and eighth day of the simulation: this phenomenon is more acute in July than in May, seemingly due to the lower temperatures encountered in May.

4. CONCLUSION

A numerical simulation model of the Bay of Biscay anchovy dynamics, under environmental influence, has been proposed. The model deals with the passive transportation period, that is the endogenous feeding period, going from birth to the resorption of the yolk-sac. The inputs of the model are data of egg concentrations and

data of physical quantities; the basic outputs are the densities of larvae coming out of the egg production, at any time and at any point of the physical space, throughout the early phase spanning from egg fertilization to the resorption of the yolk-sac. The maturation of larvae along this early phase is modelled as a function of the temperatures encountered by the larvae in the locations they are moved to and from by the currents.

Which conclusions can we draw from the simulations?

First of all, we want to underline the fact that, having described only part of the larval stage, we can hardly formulate very final conclusions. In this sense, our work is just a first step and should be followed by further steps, including the modelling of the active larval stage, the juvenile and the adult stages. Only then will it be possible to validate the model, using egg data as well as the data provided by captures. At this point, we can only offer very partial conclusions. Our claims have to be put into perspective since the domain of the simulation is not the whole Bay of Biscay, it is limited to a region around the Gironde estuary. There are other concentrations of eggs which are not included in our simulation.

It is also known that the distribution of eggs and some of the demographic and biological characteristics of both the spawners and the spawn change during the spawning season. This, obviously, was not considered here. Indeed, the validity of the simulation is limited to the days following the egg survey, and since such surveys last for a few days, it would be in principle necessary to organize the data feeding of the model accordingly.

Conclusions can be drawn from the inspection of the qualitative features shown by the simulations. The spatial egg and early larva distribution looks rather stable, both within a year and between years. Highest concentrations are located near the Gironde estuary and stay roughly in the same region during the ageing of larvae. A remark that can be made from either the cross-sections we have selected for this presentation or all of those we have examined is that there is always a 'continuity' in the variations of the colours, no jump of several orders indicating a deserted spot or on the contrary a clustering which would form in an originally homogeneous region. The initial distribution of eggs is slowly spread around, starting from its boundaries which are moving. A practical consequence of this remark could be that it would be pertinent to sample eggs and early larvae for as long as 4 to 5 d. There is not much distortion to be expected from

the initial spawns, entailed by the currents. The results on vertical diffusion, illustrated by *table 1*, indicate that sampling could be restricted to the upper part of the mixed layer.

Conclusions can be drawn from some of the statistics made on the outputs. Computations of the fractions of a 1-d cohort at a given stage have shown, first of all, that the higher the temperature the faster the eggs and larvae progress through stages. On the other hand, the difference is more marked in 1994 than in 1996, which is in agreement with the relative variations of temperatures during these years. They also showed a positive correlation between survival and the speed of maturation. Finally, estimates of age at the end of the yolk-sac stage are proposed (see section 3.3).

There are several criticisms that can be addressed to the study reported here. Let us concentrate on three: 1) the horizontal turbulence is not taken into account; 2) nor is the variability of the reproduction within a year; 3) the part of the life history modelled is very short and the results can hardly be validated.

The first criticism can be overcome: it is just a technical matter to extend the model so that the horizontal turbulence be accounted for. In fact, scale analysis can show that the impact of horizontal diffusion is generally negligible compared to the vertical diffusion. Introducing horizontal diffusion complicates enormously the mathematical handling of the problem, although it does not make too much difference in terms of numerical computations.

The criticism on the paucity of biological data is more serious: it is unlikely that data collections of breadth comparable to the one done once a year by the AZTI group could be multiplied. Below, a possible alternative, which could provide further data, is discussed.

Finally, the fact that only the passive part of the life history of the anchovy has been modelled is primarily a consequence of the present lack of data and information for the later stages of the Bay of Biscay anchovy. Prospects for going further are evoked below. We would like to point out however that simulations of the egg and early larva stages might help improve the estimations of the stock based on daily egg production, whereas present day estimates of egg productions are based on very rough models where the possible dispersion of eggs by the currents and the trajectory-induced variability in the

growth are not playing any role. We already pointed out a possible positive consequence of our simulations in justifying the scheduling of the egg sampling survey over a few days.

There is a wealth of directions to be explored and improvements to be made, in particular to overcome some of the criticisms just mentioned. It is of course necessary to describe the entire life history of the anchovy and to include the fishing and the data on the fisheries in order to validate such a model. Another direction for validating the model is to take into account the data on fish schools, whose modelling is, on the other hand, an unavoidable issue in the modelling of juvenile and adult anchovy.

Egg and larva mortality should be given special attention. As already mentioned, assuming a constant mortality is the same as having no mortality at all: we share a somewhat popular belief that mortality in this stage is the major cause of population regulation, it is likely that it affects dense subpopulations in a stronger manner than it does for less dense ones.

Heterogeneity of eggs should be given some attention. The biological quality of eggs may vary, depending on the age of the spawner and its health. Taking this variability into account would probably improve the estimates of the mortality rate of the eggs and early larvae.

The younger anchovies, those becoming adults a given year, tend to spawn later on in the year, in locations closer to the coast, than the older ones.

All these facts converge towards the same conclusion, namely that the egg distribution changes indeed a lot within a year, and thus egg surveys should be repeated accordingly. Besides the classical method used by the AZTI group whose high cost makes weekly surveys prohibitive, another method, named CUFES, is presently under development. Since CUFES only provides very partial information – the density of eggs and early larvae at a fixed depth – modelling is necessary in order to relate this partial information to the initial spawn. We are faced here with an identification problem. This question has already received some attention, and a preliminary work progress report has been made by Motos at a regional conference on oceanography of the Bay of Biscay. On the other hand, a general method for such identification of the initial spawn, based on the use of

optimal control theory, has been given by Anita and Boussouar (1999).

Acknowledgements

The research reported in this paper arose from the European project 96/048 DGXIV. It benefited from both biological and physical data, as well as discussions on several occasions with Lorenzo Motos, Andres Uriarte and their collaborators, from AZTI San Sebastian (Spain), who provided us with data from egg surveys and several enlightening discussions on biological and ecological features of the Bay of Biscay anchovy, and with Pascal Lazure, from IFREMER-Brest (France) who provided us with physical data.

REFERENCES

- Anderson, J.T., 1998. A review of size dependent survival during pre-recruit stages of fishes in relation to recruitment, *Atl. Fish. Sci.* 8, 55–66.
- Anita, S., Boussouar, A., 1999. An identification problem for an anchovy larva model. *Nonlinear Anal.* 37, 613–626.
- Bakun, A., 1985. Comparative studies and the recruitment problem: searching for generalizations. *CalCOFI Rep.* 26, 30–40.
- Bakun, A., 1996. Patterns in the Ocean: Ocean Processes and Marine Population Dynamics. Sea Grant College System, California.
- Blaxter, J.H.S., Hunter, J.R., 1982. The biology of the clupeoid fishes. *Adv. Mar. Biol.* 20, 1–223.
- Borja, A., Uriarte, A., Valencia, V., Motos, L., Uriarte, Ad., 1996. Relationships between anchovy (*Engraulis encrasicolus*) recruitment and the environment in the Bay of Biscay. *Sci. Mar.* 60 (supl. 2), 179–192.
- Cole, J., McGlade, J., 1998. Clupeoid population variability, the environment and satellite imagery in coastal upwelling systems. *Rev. Fish Biol. Fish.* 8, 445–471.
- Cury, P., Roy, C., 1989. Optimal environmental window and pelagic fish recruitment success in upwelling areas. *Can. J. Fish. Aquat. Sci.* 46, 670–680.
- Cushing, D.H., 1975. *Marine Ecology and Fisheries*. Cambridge University Press, Cambridge.
- Cushing, D.H., 1982. *Climate and Fisheries*. Academic Press, London.
- Dautray, R., Lions, J.L., 1988. *Analyse mathématique et calcul numérique pour les sciences techniques*, vol. 9. Masson.
- Eymard, R., Gallouet, T., Herbin, R., 2000. The finite volume method. In: Ciarlet, P.G., Lions, J.L. (Eds.), *Handbook of Numerical Analysis*. North-Holland, Amsterdam, pp. 723–1020.
- Garcia, A., Palomera, I., 1996. Anchovy early life history and its relation to its surrounding environment in the Western Mediterranean basin. *Sci. Mar.* 60, 155–166.
- Godunov, S.K., 1976. *Résolution des problèmes multidimensionnels de la dynamique des gaz*. Editions MIR, Moscou.
- Hjort, J., 1914. Fluctuations in the great fisheries of northern Europe viewed in the light of biological research. *Rapp. P.-v. Réunion. Cons. Perm. Int. Explor. Mer.* 19, 1–228.
- Hjort, J., 1926. Fluctuations in the year classes of important food fishes. *J. Cons. Int. Explor. Mer.* 1, 5–38.
- Hunter, J.R., Thomas, G.L., 1973. Effect of prey distribution and density on the searching and feeding behaviour of larval anchovy *Engraulis mordax* Girard. In: Blaxter, J.H.S. (Ed.), *The Early Life History of Fish*. Proc. Int. Symp. Dunstaffnag Mar. Res. Lab., Scottish Mar. Biol. Assoc., Oban, Scotland, pp. 559–574.
- Kawasaki, T., 1983. Why do some pelagic fishes have wide fluctuations in their numbers? Biological basis of fluctuation from the viewpoint of evolutionary ecology, Proceedings of the Expert Consultation to Examine Changes in Abundance and Species Composition of Neritic Fish Resources, San José, Costa Rica, 18–29 April 1983, *FAO Fisheries Report*, 291(3), pp. 1065–1080.
- Kröner, D., 1997. *Numerical Schemes for Conservation Laws*. Wiley & Teubner, New York.
- Lasker, R., 1978. The relation between oceanographic conditions and larval anchovy food in the California Current: identification of factors contributing to recruitment failure. *Rapp. P.-v. Réunion. Int. Explor. Mer.* 173, 212–230.
- Lasker, R., 1985. What limits clupeoid production? *Can. J. Fish. Aquat. Sci.* 42, 31–38.
- Lasker, R., MacCall, A.D., 1983. New ideas and fluctuations of the clupeoid stocks of California. Proceeding of the Point Oceanographic Assembly 1982 General Symposia, Canadian National Committee, Scientific Committee on Oceanic Research, Ottawa, pp. 110–120.
- Lazure, P., Jégou, A.M., 1998. 3D-modeling of seasonal evolution of Loire and Gironde plumes of Biscay bay continental shelf. *Oceanol. Acta* 21, 165–177.
- Leggett, W.C., Deblois, E., 1994. Recruitment in marine fishes: it is regulated by starvation and predation in the egg and larval stages. *Neth. J. Sea Res.* 32, 119–134.
- Lo, N.C.H., 1985. A model for temperature dependent northern anchovy egg development and an automated procedure for the assignment of age staged eggs. In: Lasker, R. (Ed.), *N.O.A.A. Technical Report NMFS*, 36, pp. 43–50.
- Mortan, K.W., 1996. *Numerical Solution of Convection-Diffusion Problems*. Chapman & Hall, London.
- Moser, H.G., Ahlstrom, E.H., 1985. Staging anchovy eggs. In: Lasker, R. (Ed.), *N.O.A.A. Technical Report NMFS*, 36, pp. 37–41.
- Motos, L., 1994. Estimacion de la biomasa desovante de la poblacion de anchoa de Vizcaya, *Engraulis encrasicolus*, a partir de su production de huevos. Bases metodologicas y aplicacion, Ph.D. thesis, Univ. Pasi Vasco Spain.
- Motos, L., 1996. Reproductive biology and fecundity of the Bay of Biscay anchovy population (*Engraulis encrasicolus* L.). *Sci. Mar.* 60 (supl. 2), 195–207.
- Motos, L., Uriarte, A., Alvarez, P., Prouzet, P., 1998. Review of the assessment of the spawning biomass of the Bay of Biscay anchovy (*Engraulis encrasicolus* L.) in 1995, 1996 and results of the 1997 survey, 1998, *ICES CM 1998/Assess:8*.

- Mullin, M.M., 1993. Webs and Scales: Physical and Ecological Process in Marine Fish Recruitment. University of Washington Press, Washington Sea Grant Program.
- Pauly, D., Tsukayam, I., 1987. The Peruvian anchoveta and its upwelling ecosystem: three decades of change. ICLARM Studies and Reviews, 15, IMARPE, Callao, Peru; GTZ, Eschborn, Germany; ICLARM, Manila, Philippines.
- Payne, A.I.L., Gulland, J.A., Brink, K.H., 1987. The Benguela and comparable ecosystems. S. Afr. J. Mar. Sci. 5, 957.
- Valvidia, J.E., 1978. The anchoveta and el niño. Rapp. P.-V. Reun. Int. Explor. Mer. 173, 196–202.
- Vignal, M.H., 1996. Convergence of a finite volume scheme for an elliptic-hyperbolic system. Model. Math. Anal. Num. 30, 841–872.
- Wroblewski, J.S., 1984. Formulation of growth and mortality of larval northern anchovy in turbulent feeding environment. Mar. Ecol. Progr. Ser. 20, 13–22.
- Wroblewski, J.S., Richman, J.G., 1987. The non-linear response of plankton to wind mixing events: implications for the survival of larval northern anchovy. J. Plankton Res. 9, 103–123.
- Wroblewski, J.S., Richman, J.G., Mellot, G.L., 1989. Optimal wind conditions for the survival of larval northern anchovy, *Engraulis mordax*: a modeling investigation. Fish. Bull. US 87, 387–398.